AMERICAN SOCIETY FOR MICROBIOLOGY | mBio®

RESEARCH ARTICLE
Molecular Biology and Physiology

The *Pseudomonas aeruginosa* Complement of Lactate Dehydrogenases Enables Use of D- and L-Lactate and Metabolic Cross-Feeding

Yu-Cheng Lin,[a] William Cole Cornell,[a] Jeanyoung Jo,[a] Alexa Price-Whelan,[a] Lars E. P. Dietrich[a]

[a]Department of Biological Sciences, Columbia University, New York, New York, USA

ABSTRACT *Pseudomonas aeruginosa* is the most common cause of chronic, biofilm-based lung infections in patients with cystic fibrosis (CF). Sputum from patients with CF has been shown to contain oxic and hypoxic subzones as well as millimolar concentrations of lactate. Here, we describe the physiological roles and expression patterns of *P. aeruginosa* lactate dehydrogenases in the contexts of different growth regimes. *P. aeruginosa* produces four enzymes annotated as lactate dehydrogenases, three of which are known to contribute to anaerobic or aerobic metabolism in liquid cultures. These three are LdhA, which reduces pyruvate to D-lactate during anaerobic survival, and LldE and LldD, which oxidize D-lactate and L-lactate, respectively, during aerobic growth. We demonstrate that the fourth enzyme, LldA, performs redundant L-lactate oxidation during growth in aerobic cultures in both a defined MOPS (morpholinepropanesulfonic acid)-based medium and synthetic CF sputum media. However, LldA differs from LldD in that its expression is induced specifically by the L-enantiomer of lactate. We also show that the *P. aeruginosa* lactate dehydrogenases perform functions in colony biofilms that are similar to their functions in liquid cultures. Finally, we provide evidence that the enzymes LdhA and LldE have the potential to support metabolic cross-feeding in biofilms, where LdhA can catalyze the production of D-lactate in the anaerobic zone, which is then used as a substrate in the aerobic zone. Together, these observations further our understanding of the metabolic pathways that can contribute to *P. aeruginosa* growth and survival during CF lung infection.

IMPORTANCE Lactate is thought to serve as a carbon and energy source during chronic infections. Sites of bacterial colonization can contain two enantiomers of lactate: the L-form, generally produced by the host, and the D-form, which is usually produced by bacteria, including the pulmonary pathogen *Pseudomonas aeruginosa*. Here, we characterize *P. aeruginosa*'s set of four enzymes that it can use to interconvert pyruvate and lactate, the functions of which depend on the availability of oxygen and specific enantiomers of lactate. We also show that anaerobic pyruvate fermentation triggers production of the aerobic D-lactate dehydrogenase in both liquid cultures and biofilms, thereby enabling metabolic cross-feeding of lactate over time and space between subpopulations of cells. These metabolic pathways might contribute to *P. aeruginosa* growth and survival in the lung.

KEYWORDS biofilms, lactate isomers, pyruvate, pyruvate fermentation

During growth and survival in communities, bacteria encounter microniches with conditions that differ from those of the external environment. Gradients form over biofilm depth due to consumption of resources by cells closer to the periphery (1–3). Efforts to control biofilm behavior in clinical and industrial settings depend on our understanding of the physiological responses to these unique conditions.

Received 1 May 2018 **Accepted** 8 August 2018 **Published** 11 September 2018

Citation Lin Y-C, Cornell WC, Jo J, Price-Whelan A, Dietrich LEP. 2018. The *Pseudomonas aeruginosa* complement of lactate dehydrogenases enables use of D- and L-lactate and metabolic cross-feeding. mBio 9:e00961-18. https://doi.org/10.1128/mBio.00961-18.

Editor Joanna B. Goldberg, Emory University School of Medicine

Address correspondence to Lars E. P. Dietrich, LDietrich@columbia.edu.

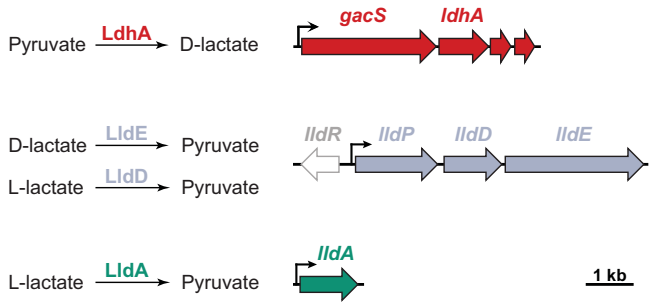

FIG 1 The *P. aeruginosa* genome encodes several enzymes that interconvert pyruvate and lactate. (Left) Reactions catalyzed by *P. aeruginosa*'s lactate dehydrogenases; (right) chromosomal loci encoding each of the corresponding enzymes. LdhA catalyzes the reduction of pyruvate during anaerobic survival. LldE catalyzes the oxidation of D-lactate during aerobic growth. Unlike *E. coli*, which contains only one gene encoding an L-lactate dehydrogenase, *P. aeruginosa* contains two orthologues for this enzyme. LldD catalyzes the oxidation of L-lactate during aerobic growth. This study describes a role for LldA in catalyzing the oxidation of L-lactate during aerobic growth.

We study the effects of biofilm resource gradients on the physiology of the opportunistic pathogen *Pseudomonas aeruginosa*, a major cause of biofilm-based infections and the most prominent cause of lung infections in patients with the inherited disease cystic fibrosis (CF) (4). *P. aeruginosa* can generate ATP for growth via oxygen and nitrate respiration and, to a limited extent, through arginine fermentation (5, 6). Sufficient ATP to support survival can be generated via (i) pyruvate fermentation (7) or (ii) cyclic reduction of endogenously produced antibiotics called phenazines, under conditions in which these compounds are reoxidized outside the cell (8, 9). We have found that some of these pathways for ATP generation also facilitate redox balancing for cells in biofilms and that *P. aeruginosa* modulates its overall community architecture in response to the availability of oxygen, nitrate, and phenazines (1, 10).

Previous work has indicated that phenazine-supported ATP generation and survival in anaerobic cell suspensions depend on reactions associated with pyruvate fermentation and oxidation (7, 9). Furthermore, lactate, a product of pyruvate fermentation, is a major component of CF sputum (11) and a significant carbon and energy source for pathogens and commensals of mammalian hosts (12–15). These observations motivated us to investigate the roles of enzymes that interconvert pyruvate and lactate in *P. aeruginosa* growth and biofilm development, including a previously uncharacterized L-lactate dehydrogenase. We found that this enzyme plays a redundant role in aerobic growth on L-lactate but that its expression is uniquely and specifically induced by the L-enantiomer of lactate, which is typically produced by plant and mammalian metabolism (16–18). Our studies also show that biofilms grown on pyruvate have the potential to engage in substrate cross-feeding, in which D-lactate produced fermentatively in the anoxic microniche acts as the electron donor for aerobic respiration in the upper, oxic portion of the biofilm. These results help us to further define potential pathways of electron flow in *P. aeruginosa* biofilm cells and the diverse metabolisms that might operate simultaneously in bacterial communities.

RESULTS AND DISCUSSION

The *P. aeruginosa* genome encodes four enzymes that interconvert pyruvate and lactate. To initiate our characterization of pathways for pyruvate and lactate utilization in *P. aeruginosa* PA14, we examined the genome for loci encoding lactate dehydrogenases. PA14 contains four genes with the following annotation: *ldhA* (PA14_52270), *lldD* (PA14_63090), *lldE* (PA14_63100), and *lldA* (PA14_33860) (Fig. 1). *ldhA* encodes a lactate dehydrogenase that reduces pyruvate to lactate during anaerobic pyruvate fermentation (7) (Fig. 1). According to computational prediction (19), *ldhA* is cotranscribed with three other genes, including that encoding the global regulator GacS. *lldD* and *lldE* encode an L-lactate dehydrogenase and a D-lactate dehydrogenase, respectively, and are cotranscribed with *lldP*, which encodes a lactate permease. *lldR*,

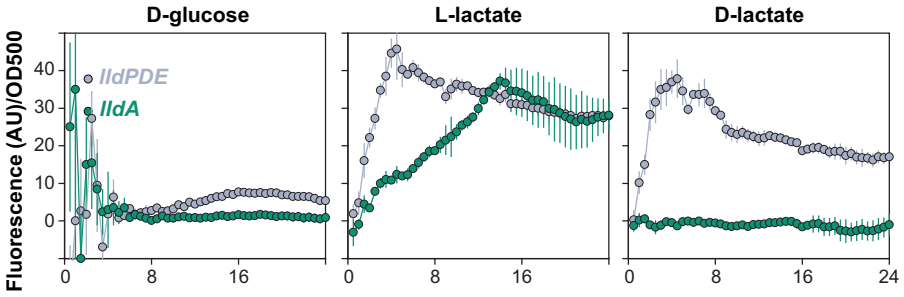

FIG 2 Expression of loci associated with pyruvate and lactate metabolism during aerobic, liquid-culture growth. Strains engineered to express GFP under the control of promoters upstream of *lldP* (which is cotranscribed with *lldD* and *lldE*) or *lldA* were grown in MOPS medium, with the indicated compounds provided as sole carbon sources. Background fluorescence from a strain with a promoterless reporter was subtracted before normalization to the OD at 500 nm. Error bars, which are often obscured by the point markers, represent the standard deviations from biological triplicates. AU, arbitrary units.

which encodes a repressor of *lldPDE* expression that is deactivated by either L- or D-lactate, lies adjacent to the *lldPDE* operon and is divergently transcribed (Fig. 1) (20). *P. aeruginosa* PA14 encodes a second, uncharacterized L-lactate dehydrogenase, called LldA, that is 44% identical to LldD. Though few other pseudomonad species contain more than one L-lactate dehydrogenase (see Fig. S1A to C in the supplemental material) (19), the *P. aeruginosa* arrangement of *lldR* and *lldPDE* (Fig. S1B) is common within the *Pseudomonas* genus. In the model organism *Escherichia coli*, by contrast, the *lldPRD* genes are arranged in an operon and *lldR* responds specifically to L-lactate (21), while the *E. coli* D-lactate dehydrogenase Dld is encoded separately (Fig. S1D) (22).

The *lldPDE* and *lldA* loci are induced by substrates of their respective protein products. Upon noticing the second gene encoding an L-lactate dehydrogenase (i.e., LldA) in the *P. aeruginosa* genome, we wondered whether we could observe its expression under conditions similar to those that induce the expression of LldD. We therefore created a suite of *P. aeruginosa* PA14 strains that express green fluorescent protein (GFP) under the control of putative promoters for lactate dehydrogenase genes. For the *lldPDE* and *lldA* reporters, we treated ~300 bp of sequence upstream of each of these loci as putative promoters. However, we viewed *ldhA* as a unique case because it was computationally predicted to be cotranscribed with *gacS*. GacS is a notorious upstream regulator of quorum sensing (23) and therefore plays a role in *P. aeruginosa* physiology distinct from that of *ldhA*. We examined transcriptome sequencing (RNA-seq) data obtained from PA14 biofilms to identify transcriptional start sites in the *gacS-ldhA* region of the genome. This profiling showed a transcriptional start site at ~46 bp upstream of the start codon of *gacS* and steady numbers of reads extending through *ldhA* (Fig. S2A), suggesting that *ldhA* expression is driven by the promoter upstream of *gacS*. Nevertheless, we created reporter strains that contained portions of sequence from the regions upstream of either *gacS* or *ldhA*, respectively, so that we could detect any potential, independent expression of *ldhA*.

The reporter strains were grown aerobically in defined media. We observed very low levels of expression from the *gacS* promoter, but not the putative *ldhA* promoter region, as predicted from the RNA-seq profiling (Fig. S2B). Cotranscription of *gacS* and *ldhA* makes physiological sense in that the high cell density associated with quorum sensing leads to oxygen limitation and therefore a condition in which cells potentially benefit from pyruvate fermentation. A low level of expression was also observed after ~9 h of growth for *lldPDE*, but not *lldA*, on D-glucose (left panel of Fig. 2). *lldPDE* expression was strongly induced from the start of growth and peaked around 4 h, when either D- or L-lactate was provided as the sole carbon source (middle and right panels of Fig. 2). These results are consistent with a previous study of *P. aeruginosa* XMG (20), which showed that LldR responds to both enantiomers of lactate. In contrast, *lldA* expression was not observed on D-glucose or D-lactate and was induced strictly by

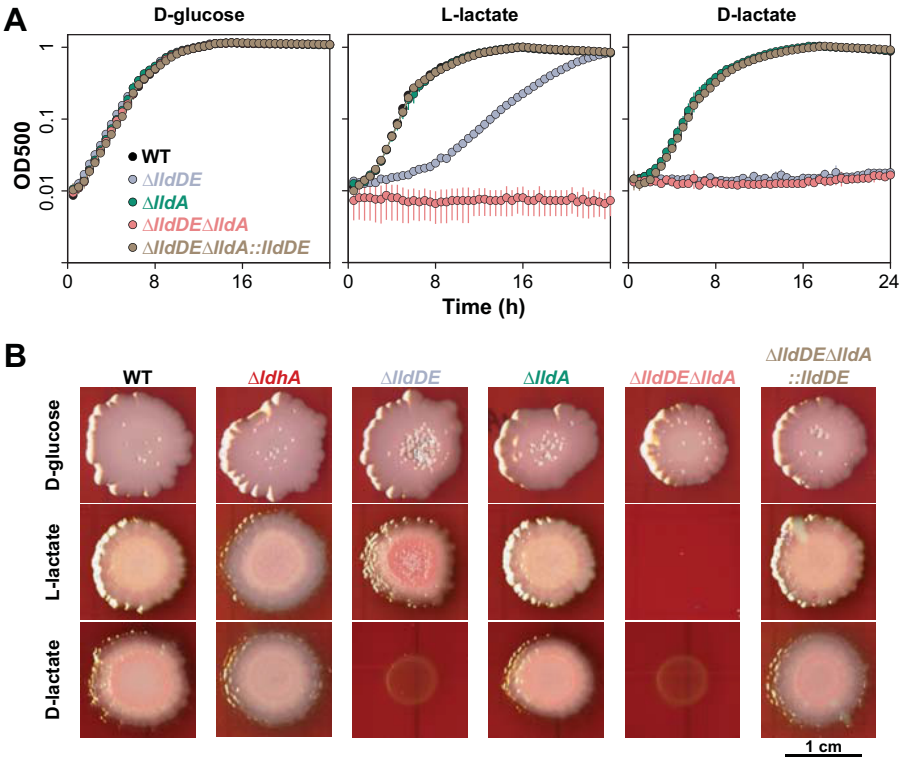

FIG 3 Physiological roles of enzymes that interconvert pyruvate and lactate during growth in shaken liquid cultures and biofilms. (A) Aerobic growth of the indicated strains in MOPS medium with D-glucose, L-lactate, or D-lactate provided as the sole carbon source. Error bars, which are obscured by the point marker in most cases, represent the standard deviations from biological triplicates. (B) Growth and morphological development of the indicated strains under an oxic atmosphere on MOPS medium containing the dyes Congo red and Coomassie blue and amended with D-glucose, L-lactate, or D-lactate. Images were taken after 4 days of incubation. WT, wild type.

L-lactate (Fig. 2). This finding is consistent with LldA's predicted physiological function and indicates that it is controlled by a regulator that specifically senses the L-enantiomer. In contrast to that of *lldPDE*, *lldA* expression showed a more gradual increase over the first several hours of growth and peaked at around 14 h.

Both LldD and LldA contribute to L-lactate utilization during liquid-culture and biofilm growth. To test whether LldA contributes uniquely to L-lactate utilization, we generated deletion strains lacking *lldDE*, *lldA*, or both loci and tested their abilities to grow aerobically in defined media. When L-lactate was provided as the sole carbon source, deletion of *lldDE* did not completely abolish growth but rather led to biphasic growth at lower rates than that observed for the wild type (Fig. 3A). This slow growth of the Δ*lldDE* mutant on L-lactate contrasts with that seen for an equivalent mutant created in *Pseudomonas stutzeri* SDM, which shows no growth on L-lactate (24), and indicates that LldD is not the only enzyme that oxidizes L-lactate in *P. aeruginosa*. Indeed, deletion of *lldA* in the Δ*lldDE* background yielded a strain that was completely defective in growth on L-lactate (Fig. 3A). However, the Δ*lldA* single deletion did not result in any growth defect on L-lactate (Fig. 3A), suggesting that LldA's activity is redundant with that of LldD. Consistent with findings reported for *P. stutzeri* SDM (24), we found that *lldDE* was necessary for growth with D-lactate (Fig. 3A), indicating that LldE is the only enzyme that oxidizes this enantiomer of lactate during aerobic growth.

The D- and L-enantiomers of lactate are generally associated with bacterial and metazoan metabolism, respectively, with L-lactate being the primary form produced in sites of microbial colonization, such as the mammalian gut (13) and the airways of patients with CF (25). We were therefore interested in the relevance of lactate dehydrogenase activity to the growth and morphogenesis of biofilms, which represent a

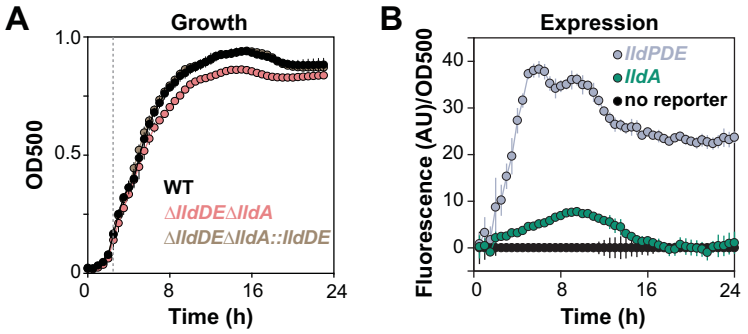

FIG 4 PA14 utilizes the L-lactate in synthetic cystic fibrosis sputum medium (SCFM) for growth. (A) Growth of the indicated strains in SCFM. Error bars represent the standard deviations from at least four biological replicates and are omitted in cases where they would be obscured by point markers. *P* values of the Δ*lldDE* Δ*lldA* double mutant versus the wild type and Δ*lldDE* Δ*lldA*::*lldDE* strain are <0.0001 based on an unpaired, two-tailed *t* test. (B) Expression of the indicated reporter constructs in SCFM. Background fluorescence from a strain with a promoterless reporter was subtracted before normalization to the OD at 500 nm.

major lifestyle assumed by commensal and pathogenic bacteria. To examine this, we grew deletion mutants lacking lactate dehydrogenase genes as colony biofilms on defined media containing the dyes Congo red and Coomassie blue, which aid visualization of morphogenetic features. Generally, the colony biofilm phenotypes of the mutants matched phenotypes observed during aerobic growth in liquid cultures (Fig. 3B). The lack of an effect of *ldhA* deletion (Fig. 3B) under these conditions is consistent with the role of LdhA as a pyruvate reductase (7). We note that, in addition to having its expected, moderate growth defect on L-lactate, the Δ*lldDE* mutant showed increased production of matrix (as indicated by increased binding of Congo red) (Fig. 3B). In other work (1), we have found that this phenotype often correlates with impaired redox balancing and a reduced cellular redox state; in this case, therefore, it might indicate that the LldA enzyme does not sufficiently support the maintenance of redox homeostasis in colony biofilms.

The L-lactate in synthetic cystic fibrosis media contributes to PA14 growth. Lactate is a major component of CF sputum (11), and its concentration correlates with the exacerbation of chronic infections in CF lungs (25). We predicted that LldD and/or LldA would contribute to PA14 growth in synthetic CF sputum media (11, 26, 27), which contain millimolar concentrations of L-lactate. We grew mutants lacking these L-lactate dehydrogenases in three different media that imitate nutrient availability in CF lungs: (i) synthetic CF sputum medium (SCFM), (ii) modified artificial sputum medium (ASMDM, which is similar to SCFM but also contains bovine serum albumin [BSA], mucin, and herring sperm DNA), and (iii) SCFM2, which is similar to ASMDM but contains additional large molecules. We found that the Δ*lldDE* Δ*lldA* double mutant, which is not able to grow using L-lactate as a sole carbon source (Fig. 3), showed an ~10% decrease in growth (Fig. 4A) in SCFM, which was evident after cultures entered late stationary phase (Fig. 4A and S3). Both *lldPDE* and *lldA* were transcriptionally induced in SCFM, though *lldPDE* was expressed at a higher level than *lldA* (Fig. 4B). We also detected a marked defect for the double mutant in ASMDM, though interestingly, it occurred earlier in the growth curve (Fig. S3). A modest defect was also detectable in SCFM2 (Fig. S3). These results suggest that LldD and LldA together might contribute to L-lactate utilization for growth in the CF lung environment. Our observations indicate that lactate dehydrogenases make less significant contributions to growth in a more complex medium containing some of the large molecules and polymers available in this setting; however, the CF lung environment is heterogeneous and might nevertheless contain subregions where lactate is a major source of carbon and energy.

LldE supports the growth of PA14 on self-produced D-lactate. The fact that the *P. aeruginosa* genome encodes enzymes that catalyze the oxygen-dependent intercon-

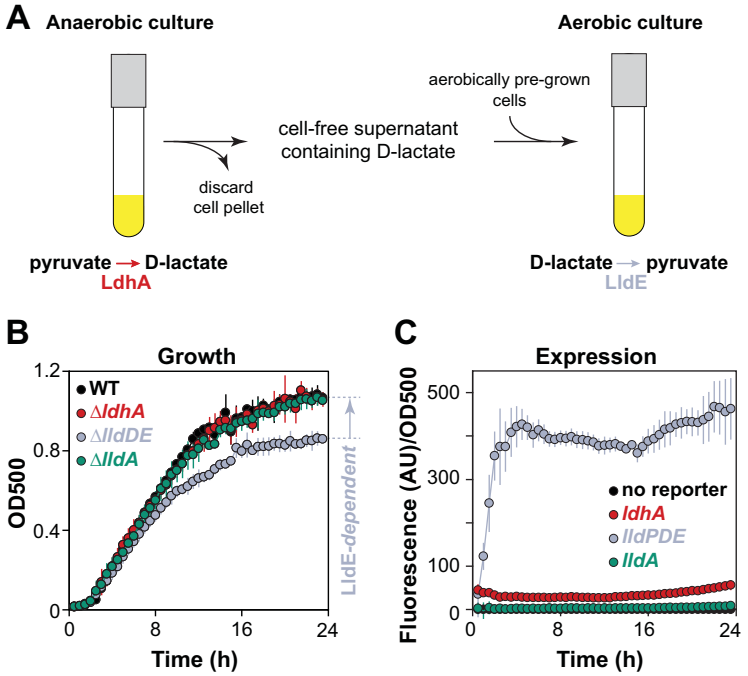

FIG 5 Growth of PA14 on self-produced D-lactate. (A) Design schematic for a pyruvate/D-lactate cross-feeding experiment in liquid cultures. *P. aeruginosa* PA14 was incubated in anoxic liquid medium (MOPS plus 0.1% tryptone plus 40 mM sodium pyruvate) to promote the fermentation and production of D-lactate. The supernatants collected from these cultures were used as the growth medium for oxic cultures, in which the D-lactate then served as a carbon source for PA14 growth. (B) Growth of the indicated strains on supernatants obtained from anaerobic cultures that had fermented pyruvate. Error bars represent the standard deviations from three biological replicates. *P* values for the Δ*lldDE* mutant versus the wild type, Δ*lldA* mutant, and Δ*ldhA* mutant are 4.6×10^{-4}, 2.2×10^{-4}, and 1.1×10^{-3}, respectively, and are based on unpaired, two-tailed *t* test results with equal variances. (C) Expression of the indicated reporter constructs during growth on the supernatant described in panel A. Background fluorescence from a strain with a promoterless reporter was subtracted before normalization to the OD at 500 nm.

version of pyruvate and D-lactate raises the possibility that cells in environments where oxygen availability varies over time or space engage in metabolic cross-feeding. In this scenario, pyruvate is reduced to D-lactate under anoxic conditions, and then D-lactate is oxidized to pyruvate and further metabolized under oxic conditions. We set out to test this possibility in liquid cultures by first incubating *P. aeruginosa* anaerobically with pyruvate (to stimulate D-lactate production) and then using the supernatant from these cultures as the medium for aerobic growth of fresh cultures (which should use the D-lactate in an *lldE*-dependent manner) (Fig. 5A). First, we verified that *ldhA* supports the survival of PA14 under anaerobic conditions in which pyruvate is provided as the major carbon source (Fig. S4). We found that this phenomenon required the inclusion of a complex nutrient source (e.g., lysogeny broth [LB] or tryptone) in the medium, possibly as a source of an unidentified cofactor used in pyruvate fermentation. We therefore carried out a series of titration experiments in order to identify a concentration of tryptone that would allow us to observe *lldE*-dependent growth (Fig. S5A) and *lldPDE* expression (Fig. S5B) at concentrations of lactate that could be produced in the pyruvate fermentation cultures (7). Next, we incubated PA14 cells for 7 days in anoxic liquid 0.1% tryptone medium containing 40 mM pyruvate, collected cell-free spent medium from these cultures, and used it as the growth medium for freshly inoculated aerobic cultures (Fig. 5A). Consistent with the model in which PA14-generated D-lactate was present in the medium and acted as a carbon source (Fig. 5A), this experimental design yielded high levels of expression from the *lldPDE* reporter (Fig. 5C) and revealed a growth defect for the Δ*lldDE* mutant (Fig. 5B).

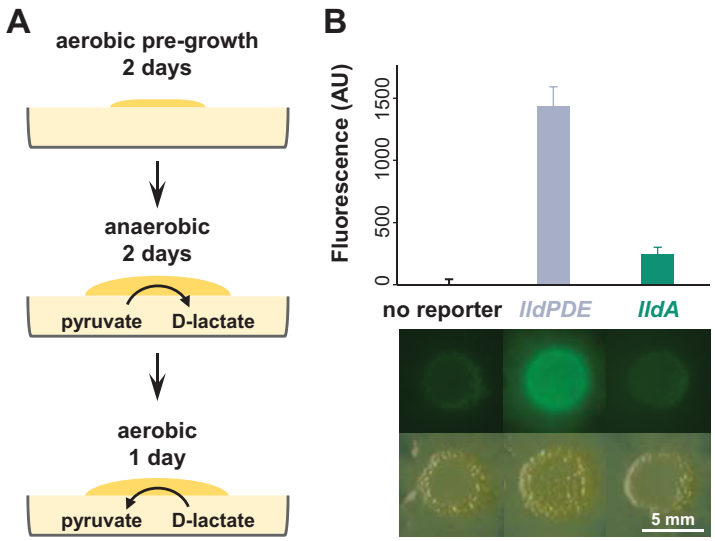

FIG 6 Self-produced D-lactate induces *lldPDE* in biofilms. (A) Design schematic for a pyruvate/D-lactate cross-feeding experiment in liquid cultures in colony biofilms. Colonies were initially grown atop filter membranes on plates containing 1% tryptone, 1% agar plus 40 mM sodium pyruvate for 2 days under an oxic atmosphere to establish biomass and then transferred to fresh plates of medium containing 0.1% tryptone, 1% agar plus 40 mM sodium pyruvate in an anoxic chamber to stimulate pyruvate fermentation and D-lactate production for 2 days. Finally, the plates were moved from the chamber and back into an oxic atmosphere for 1 day. The procedure was carried out at room temperature. (B) Fluorescence quantification (top) and images (bottom) of colonies grown using the procedure shown in panel A. Background fluorescence was normalized to the "no reporter" control. Error bars represent the standard deviations from three biological replicates. *P* values for lldPDE reporter versus no reporter and lldA reporter are 1.0×10^{-4} and 2.3×10^{-4}, respectively, and are based on unpaired, two-tailed *t* test results with equal variance.

We next asked whether PA14 has the potential to utilize self-produced D-lactate during growth in colony biofilms. Colony biofilms were first grown aerobically on pyruvate for 2 days to establish sufficient biomass and then transferred to fresh anoxic plates for 2 days to promote pyruvate fermentation and D-lactate production. These plates were then subsequently moved to oxic conditions and incubated for 1 day (Fig. 6A). This procedure yielded high expression of the *lldPDE* reporter (controlled by an L- and D-lactate sensor) but not the *lldA* reporter (controlled by an L-lactate-specific sensor) (Fig. 6B), indicating the presence of self-produced D-lactate, which might potentially be utilized by PA14 in colony biofilms.

***P. aeruginosa* PA14 cells in biofilms have the potential to engage in pyruvate/lactate cross-feeding over the oxygen gradient.** As PA14 colony biofilms increase in thickness, they develop steep oxygen gradients, leading to the formation of metabolic subpopulations in oxic and anoxic zones (28). After observing that PA14 could produce D-lactate under fermentative conditions that acts as an electron donor for aerobic growth, we hypothesized that pyruvate fermentation and aerobic D-lactate utilization cooccur in biofilms. To test this, we grew colony biofilms on medium with and without pyruvate and examined the expression of the *lldPDE* operon, which is induced by D-lactate. We observed higher expression of *lldPDE* when colonies were grown on medium containing pyruvate (Fig. 7A), indicating that cells in the anoxic zone carried out pyruvate fermentation and produced D-lactate. These results suggest that, in addition to generating ATP and supporting survival for cells in oxygen-limited regions of biofilms, pyruvate fermentation can serve to produce D-lactate that supports growth in regions where oxygen is available (Fig. 7B). Overall, they add a layer of complexity to our picture of the integrated metabolisms occurring in physiologically heterogeneous bacterial communities.

Concluding remarks. Metabolic cross-feeding has been described for polymicrobial communities that are models for those found within the human body and that colonize

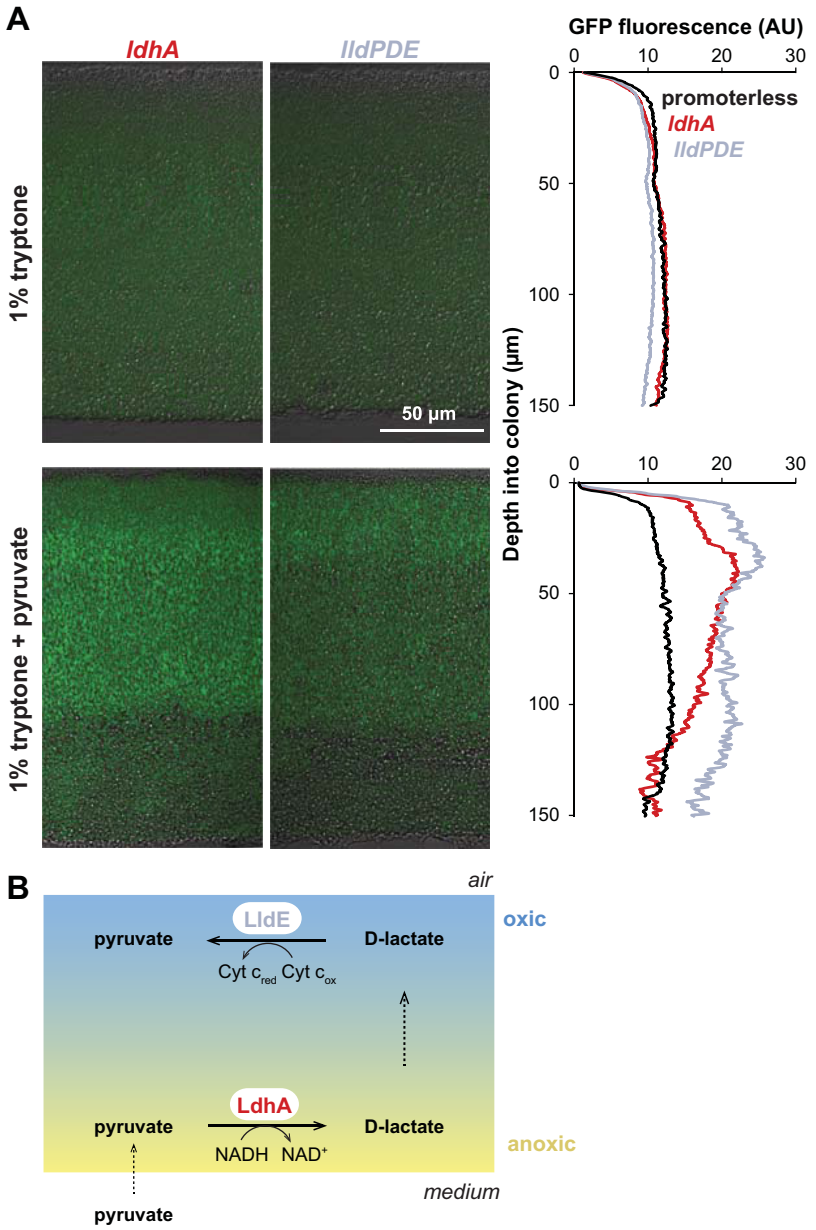

FIG 7 Expression of enzymes for interconversion of pyruvate and lactate over biofilm depth. Expression of *ldhA* (which catalyzes pyruvate reduction under anaerobic conditions) and *lldE* (which catalyzes D-lactate oxidation under aerobic conditions) as reported by promoter-*gfp* fusions in thin sections from wild-type PA14 biofilms. Biofilms were grown for 3 days on 1% tryptone medium with or without 10 mM pyruvate. Quantification of fluorescence over depth is shown at the right. This experiment was repeated in biological triplicate, and representative results are shown. Cyt c_{red}, with reduced cytochrome *c*; Cyt c_{ox}, with oxidized cytochrome *c*.

sites such as the oral cavity and large intestine (29, 30). Our findings indicate that metabolic cross-feeding might take place in a single-species biofilm and arise from physiological heterogeneity, in which a fermentation product formed in the anaerobic microniche is oxidized by cells in the aerobic microniche. Our model for this cross-feeding in biofilms might be viewed as a form of electron shuttling (Fig. 7B), with the role of D-lactate as an electron carrier between anoxic and oxic subzones showing some similarities to that of phenazines (1, 8, 28).

Most pseudomonad species have either *lldD* or *lldA* for L-lactate utilization (Fig. S1C). We have shown that in *P. aeruginosa* PA14, *lldD* and the previously uncharacterized

orphan *lldA* encode L-lactate dehydrogenases with redundant functions during growth in liquid cultures. However, *lldA* differs from *lldD* in that it is specifically induced by L-lactate. The presence of redundant L-lactate dehydrogenases in *P. aeruginosa* may represent an adaptation to the host environment, given the fact that host organisms, such as humans and plants (18, 31, 32), produce primarily the L-enantiomer. Several studies have implicated L-lactate metabolism in bacterial virulence during infections, including *Salmonella*-induced gastroenteritis (13) and gonococcal infection of the genital tract (12). Our results suggest that LldD and LldA utilize L-lactate in SCFM and other artificial sputum media to promote PA14 growth (Fig. 4A and Fig. S3). Similarly, other common CF pathogens encode L-lactate dehydrogenases homologous to LldD and LldA. Using the *P. aeruginosa* PA14 LldD, LldA, and LldE protein sequences, we searched for homologues in representative strains of *Achromobacter xylosoxidans*, *Burkholderia multivorans*, *Haemophilus influenzae*, and *Stenotrophomonas maltophilia* (33–35). We found that *H. influenzae* and *S. maltophilia* contain an L-lactate dehydrogenase homolog but that *A. xylosoxidans* and *B. multivorans*, like *P. aeruginosa*, contain multiple homologs. As L-lactate is a significant metabolite available in the lungs of CF patients (11, 25, 36, 37), these enzymes may contribute to the abilities of *P. aeruginosa* and other pathogens to colonize and persist in this environment.

MATERIALS AND METHODS

Bacterial strains and growth conditions. Unless otherwise indicated, *P. aeruginosa* strain UCBPP-PA14 and mutants thereof (38) were routinely grown in lysogeny broth (LB; 1% tryptone, 1% NaCl, 0.5% yeast extract) (39) at 37°C with shaking at 250 rpm. Overnight cultures were grown for 16 ± 1 h. For genetic manipulation, strains were typically grown on LB solidified with 1.5% agar. Strains used in this study are listed in Table S1 in the supplemental material. In general, liquid precultures served as inocula for experiments. Overnight precultures for biological replicates were started from separate clonal colonies on streak plates.

Construction of mutant *P. aeruginosa* strains. For making markerless deletion mutants in *P. aeruginosa* PA14 (Table S1), ~1-kb flanking sequences from each side of the target gene were amplified using the primers listed in Table S2 and inserted into the allelic-replacement vector pMQ30 through gap repair cloning in *Saccharomyces cerevisiae* InvSc1 (40). Each plasmid listed in Table S1 was transformed into *Escherichia coli* strain UQ950, verified by sequencing, and moved into PA14 using biparental conjugation. PA14 single recombinants were selected on LB agar plates containing 100 μg/ml gentamicin. Double recombinants (markerless deletions) were selected on sucrose plates (1% tryptone, 0.5% yeast extract, 10% sucrose, and 1.5% agar). Genotypes of deletion mutants were verified by PCR. Combinatorial mutants were constructed by using single mutants as parent strains.

Construction of GFP reporter strains. Transcriptional reporter constructs for the genes *ldhA*, *gacS*, *lldP*, and *lldA* were made by fusing their promoter sequences with *gfp* using primers listed in Table S2. Respective primers were used to amplify promoter regions (as indicated in Table S1) and to add an SpeI digest site to the 5′ end of the promoter and an XhoI digest site to its 3′ end. For the *ldhA* reporter, an EcoRI site was used instead of XhoI. Purified PCR products were digested and ligated into the multiple-cloning site (MCS) upstream of the *gfp* sequence of pLD2722, which is a derivative of pYL122 (41) and contains a ribosome-binding site between the MCS and *gfp*. Plasmids were transformed into *E. coli* strain UQ950, verified by sequencing, and moved into PA14 using biparental conjugation. Conjugative transfer of pLD2722 was conducted with the *E. coli strain* S17-1 (41). PA14 single recombinants were selected on M9 minimal medium agar plates (47.8 mM Na_2HPO_4, 22 mM KH_2PO_4, 8.6 mM NaCl, 18.6 mM NH_4Cl, 1 mM $MgSO_4$, 0.1 mM $CaCl_2$, 20 mM sodium citrate dihydrate, 1.5% agar) containing 70 μg/ml gentamicin. The plasmid backbone of pLD2722 was resolved from PA14 using Flp-Flp recombination target (FRT) recombination by introduction of the pFLP2 plasmid (42) and selected on M9 minimal medium agar plates containing 300 μg/ml carbenicillin and further on sucrose plates (1% tryptone, 0.5% yeast extract, 10% sucrose, 1.5% agar). The presence of *gfp* in the final clones was confirmed by PCR.

Liquid-culture growth assays. Overnight (16-h) precultures were diluted 1:100 in a clear-bottom, polystyrene black 96-well plate (VWR 82050-756), with each well containing 200 μl of medium. Cultures were then incubated at 37°C with continuous shaking at medium speed in a BioTek Synergy 4 plate reader. Reporter strains were grown in MOPS medium (50 mM MOPS, 43 mM NaCl, 93 mM NH_4Cl, 2.2 mM KH_2PO_4, 1 mM $MgSO_4$, 1 μg/ml $FeSO_4$ at pH 7.0) amended with one of the following carbon sources: 20 mM D-glucose, 40 mM L-lactate, or 40 mM D-lactate (Sigma-Aldrich). Expression of GFP was assessed by taking fluorescence readings at excitation and emission wavelengths of 480 nm and 510 nm, respectively, every 30 min for up to 24 h. Growth was assessed by taking readings of optical density at 500 nm (OD_{500}) simultaneously with the fluorescence readings.

Colony growth assays. Overnight (16-h) precultures were diluted 1:10 in phosphate-buffered saline (PBS). Five microliters of diluted cultures was spotted onto MOPS medium (50 mM MOPS, 43 mM NaCl, 93 mM NH_4Cl, 2.2 mM KH_2PO_4, 1 mM $MgSO_4$, 1 μg/ml $FeSO_4$ at pH 7.0) amended with one of the following carbon sources: 20 mM D-glucose, 40 mM L-lactate, or 40 mM D-lactate (Sigma-Aldrich). The culture medium was then solidified with 1% agar (Teknova). Colonies were incubated at 25°C for up to

4 days and imaged with an Epson Expression 11000XL scanner. Fluorescence images (Fig. 6B) were taken with a Zeiss Axio Zoom.V16 microscope (excitation, 488 nm; emission, 509 nm for imaging of GFP fluorescence).

Anaerobic survival assays. For each anaerobic liquid sample, 50 μl of overnight (16-h) precultures were diluted in 5 ml of potassium phosphate (100 mM)-buffered (pH 7.4) LB (7, 43) in a Balch tube and then incubated at 37°C with shaking at 250 rpm for 2.5 h to early to mid-exponential phase (OD_{500}, ~0.5). Balch tubes containing subcultures were then transferred into the anaerobic chamber (80% N_2, 15% CO_2, and 5% H_2) and sealed with rubber stoppers to maintain anoxia. Anaerobic tubes were incubated with shaking at 250 rpm at 37°C throughout the period of the survival assay. To measure CFU from the anaerobic culture, 10 to 50 μl of culture was aspirated from the tube with a 1-ml syringe (Care Touch) fitted with a 23-gauge needle (Becton, Dickinson), and then serially diluted in LB down to 10^{-6} CFU and plated on 1% tryptone plates for CFU counting.

Thin sectioning and preparation for microscopic analyses. Thin sections of *P. aeruginosa* colonies were prepared as described previously (44). Briefly, to produce bilayer plates, a 4.5-mm-thick bottom layer of medium (1% agar,1% tryptone) was poured and allowed to solidify before a 1.5-mm-thick top layer was poured. Precultures were incubated overnight, diluted 1:100 in LB, and incubated until early to mid-exponential phase (OD_{500}, ~0.5). Five microliters of culture were spotted onto the top agar layer and incubated in the dark at 25°C with >90% humidity (Percival CU-22L) for up to 3 days. Colonies were sacrificed for thin sectioning at specified time points by first covering them with a 1.5-mm-thick layer of 1% agar, which sandwiches each colony between two 1.5-mm layers of solidified agar. Sandwiched colonies were lifted from the bottom layer of agar and soaked in 50 mM L-lysine in PBS (pH 7.4) at 4°C for 4 h, fixed in 4% formaldehyde–50 mM L-lysine–PBS (pH 7.4) at 4°C for 4 h, and then incubated in the fixative overnight at 37°C. Fixed colonies were washed twice in PBS and dehydrated through a series of ethanol washes (25%, 50%, 70%, and 95% ethanol in PBS and 3 times with 100% ethanol) for 1 h each and then cleared by means of three 1-h washes in Histo-Clear-II (National Diagnostics HS-202). Cleared colonies were infiltrated with paraffin wax (Electron Microscopy Sciences; Fisher Scientific 50-276-89) at 55°C twice for 2 h each. Infiltrated colonies were solidified by overnight incubation at 4°C. Sections were cut perpendicularly to the base of the colony in 10-μm slices using an automatic microtome (Thermo Fisher Scientific 905200ER), floated over a water bath at 45°C, collected onto slides, and air-dried overnight. Dried slides were heat-fixed on a hotplate at 45°C for 1 h and then rehydrated to PBS by reversing the dehydration steps listed above. Sections were then immediately mounted beneath a coverslip in Tris-buffered DAPI (4′,6-diamidino-2-phenylindole)–Fluoro-Gel (Electron Microscopy Sciences; Fisher Scientific 50-246-93). Differential interference contrast (DIC) and fluorescent confocal images were captured for at least three biological replicates of each strain using an LSM700 confocal microscope (Zeiss).

RNA-seq analysis. Δ*phz* (45) colonies were grown on filter membranes (0.2-μm pore size, 25-mm diameter; Whatman) placed on 1% tryptone, 1.5% agar at 25°C for 76 h. Colonies were treated with RNAprotect bacterial reagent (Qiagen), samples were excised by microscopic laser dissection, and RNA was extracted using the RNeasy plant minikit (Qiagen). RNA samples were processed by Genewiz, including rRNA depletion and dUTP incorporation for strand-specific sequencing (Illumina HiSeq 2500 platform). Sixteen fastq files were mapped to the reference PA14 genome using Bowtie2 (46) with an ~97% success rate to generate SAM (sequence alignment map) files. SAM files containing ~2 × 108 reads in total were merged, sorted, and indexed with SAMtools (47). Read coverage was visualized with Integrative Genomics Viewer (IGV) software (48).

Preparation of synthetic SCFM and derivatives. Cystic fibrosis sputum medium (SCFM) was prepared as described previously (11). SCFM contains the following ingredients: 2.28 mM NH_4Cl, 14.94 mM KCl, 51.85 mM NaCl, 10 mM MOPS, 1.3 mM NaH_2PO_4, 1.25 mM Na_2HPO_4, 0.348 mM KNO_3, 0.271 mM K_2SO_4, 1.754 mM $CaCl_2$, 0.606 mM $MgCl_2$, 0.0036 mM $FeSO_4$, 3 mM D-glucose, 9.3 mM sodium L-lactate, 0.827 mM L-aspartate, 1.072 mM L-threonine, 1.446 mM L-serine, 1.549 mM L-glutamate·HCl, 1.661 mM L-proline, 1.203 mM glycine, 1.78 mM L-alanine, 0.16 mM L-cysteine·HCl, 1.117 mM L-valine, 0.633 mM L-methionine, 1.12 mM L-isoleucine, 1.609 mM L-leucine, 0.802 mM L-tyrosine, 0.53 mM L-phenylalanine, 0.676 mM L-ornithine·HCl, 2.128 mM L-lysine·HCl, 0.519 mM L-histidine·HCl, 0.013 mM L-tryptophan, and 0.306 mM L-arginine·HCl. Depending on the solubility of the various salts, concentrations of their stock solutions ranged from 0.2 M to 1 M. Stock concentrations for D-glucose and sodium L-lactate were 1 M and for amino acid stocks 0.1 mM. No stock solution was prepared for L-tyrosine or L-tryptophan due to poor solubility. The pH of SCFM was adjusted to 6.5 with KOH and sterilized by filtration (Thermo Scientific Nalgene Rapid-Flow). ASMDM was prepared as previously described (26) by supplementing SCFM with 10 mg/ml bovine serum albumin, 10 mg/ml mucin from porcine stomach, and 1.4 mg/ml herring sperm DNA. SCFM2 was prepared by supplementing SCFM with 5 mg/ml mucin from porcine stomach, 100 μg/ml 1,2-dioleoyl-*sn*-glycero-3-phosphocholine (DOPC), 300 μM *N*-acetyl-D-glucosamine, and 600 μg/ml herring sperm DNA as previously described (27).

SUPPLEMENTAL MATERIAL

Supplemental material for this article may be found at https://doi.org/10.1128/mBio.00961-18.

FIG S1, EPS file, 1.6 MB.

FIG S2, EPS file, 1.8 MB.

FIG S3, EPS file, 2.1 MB.

FIG S4, EPS file, 1.2 MB.

FIG S5, EPS file, 2.2 MB.
TABLE S1, PDF file, 0.3 MB.
TABLE S2, PDF file, 0.1 MB.

ACKNOWLEDGMENTS

This work was supported by NIH/NIAID grant R01AI103369, an NSF Career Award to L.E.P.D., and NIH training grant 5T32GM008798 to J.J.

REFERENCES

1. Dietrich LEP, Okegbe C, Price-Whelan A, Sakhtah H, Hunter RC, Newman DK. 2013. Bacterial community morphogenesis is intimately linked to the intracellular redox state. J Bacteriol 195:1371–1380. https://doi.org/10.1128/JB.02273-12.
2. Stewart PS, Zhang T, Xu R, Pitts B, Walters MC, Roe F, Kikhney J, Moter A. 2016. Reaction-diffusion theory explains hypoxia and heterogeneous growth within microbial biofilms associated with chronic infections. NPJ Biofilms Microbiomes 2:16012. https://doi.org/10.1038/npjbiofilms.2016.12.
3. Kempes CP, Okegbe C, Mears-Clarke Z, Follows MJ, Dietrich LEP. 2014. Morphological optimization for access to dual oxidants in biofilms. Proc Natl Acad Sci U S A 111:208–213. https://doi.org/10.1073/pnas.1315521110.
4. de Koff EM, de Winter-de Groot KM, Bogaert D. 2016. Development of the respiratory tract microbiota in cystic fibrosis. Curr Opin Pulm Med 22:623–628. https://doi.org/10.1097/MCP.0000000000000316.
5. Williams HD, Zlosnik JEA, Ryall B. 2007. Oxygen, cyanide and energy generation in the cystic fibrosis pathogen Pseudomonas aeruginosa. Adv Microb Physiol 52:1–71.
6. Lüthi E, Mercenier A, Haas D. 1986. The arcABC operon required for fermentative growth of Pseudomonas aeruginosa on arginine: Tn5-751-assisted cloning and localization of structural genes. J Gen Microbiol 132:2667–2675. https://doi.org/10.1099/00221287-132-10-2667.
7. Eschbach M, Schreiber K, Trunk K, Buer J, Jahn D, Schobert M. 2004. Long-term anaerobic survival of the opportunistic pathogen Pseudomonas aeruginosa via pyruvate fermentation. J Bacteriol 186:4596–4604. https://doi.org/10.1128/JB.186.14.4596-4604.2004.
8. Wang Y, Kern SE, Newman DK. 2010. Endogenous phenazine antibiotics promote anaerobic survival of Pseudomonas aeruginosa via extracellular electron transfer. J Bacteriol 192:365–369. https://doi.org/10.1128/JB.01188-09.
9. Glasser NR, Kern SE, Newman DK. 2014. Phenazine redox cycling enhances anaerobic survival in Pseudomonas aeruginosa by facilitating generation of ATP and a proton-motive force. Mol Microbiol 92:399–412. https://doi.org/10.1111/mmi.12566.
10. Madsen JS, Lin Y-C, Squyres GR, Price-Whelan A, de Santiago Torio A, Song A, Cornell WC, Sørensen SJ, Xavier JB, Dietrich LEP. 2015. Facultative control of matrix production optimizes competitive fitness in Pseudomonas aeruginosa PA14 biofilm models. Appl Environ Microbiol 81:8414–8426. https://doi.org/10.1128/AEM.02628-15.
11. Palmer KL, Aye LM, Whiteley M. 2007. Nutritional cues control Pseudomonas aeruginosa multicellular behavior in cystic fibrosis sputum. J Bacteriol 189:8079–8087. https://doi.org/10.1128/JB.01138-07.
12. Exley RM, Wu H, Shaw J, Schneider MC, Smith H, Jerse AE, Tang CM. 2007. Lactate acquisition promotes successful colonization of the murine genital tract by Neisseria gonorrhoeae. Infect Immun 75:1318–1324. https://doi.org/10.1128/IAI.01530-06.
13. Gillis CC, Hughes ER, Spiga L, Winter MG, Zhu W, Furtado de Carvalho T, Chanin RB, Behrendt CL, Hooper LV, Santos RL, Winter SE. 2018. Dysbiosis-associated change in host metabolism generates lactate to support salmonella growth. Cell Host Microbe 23:54–64.e6. https://doi.org/10.1016/j.chom.2017.11.006.
14. Jiang T, Gao C, Ma C, Xu P. 2014. Microbial lactate utilization: enzymes, pathogenesis, and regulation. Trends Microbiol 22:589–599. https://doi.org/10.1016/j.tim.2014.05.008.
15. Lichtenegger S, Bina I, Roier S, Bauernfeind S, Keidel K, Schild S, Anthony M, Reidl J. 2014. Characterization of lactate utilization and its implication on the physiology of Haemophilus influenzae. Int J Med Microbiol 304:490–498. https://doi.org/10.1016/j.ijmm.2014.02.010.
16. Petersen C. 2005. D-Lactic acidosis. Nutr Clin Pract 20:634–645. https://doi.org/10.1177/0115426505020006634.
17. Kowlgi NG, Chhabra L. 2015. D-Lactic acidosis: an underrecognized complication of short bowel syndrome. Gastroenterol Res Pract 2015:476215. https://doi.org/10.1155/2015/476215.
18. Maurino VG, Engqvist MKM. 2015. 2-Hydroxy acids in plant metabolism. Arabidopsis Book 13:e0182. https://doi.org/10.1199/tab.0182.
19. Winsor GL, Griffiths EJ, Lo R, Dhillon BK, Shay JA, Brinkman FSL. 2016. Enhanced annotations and features for comparing thousands of pseudomonas genomes in the pseudomonas genome database. Nucleic Acids Res 44:D646–D653. https://doi.org/10.1093/nar/gkv1227.
20. Gao C, Hu C, Zheng Z, Ma C, Jiang T, Dou P, Zhang W, Che B, Wang Y, Lv M, Xu P. 2012. Lactate utilization is regulated by the FadR-type regulator LldR in Pseudomonas aeruginosa. J Bacteriol 194:2687–2692. https://doi.org/10.1128/JB.06579-11.
21. Goers L, Ainsworth C, Goey CH, Kontoravdi C, Freemont PS, Polizzi KM. 2017. Whole-cell Escherichia coli lactate biosensor for monitoring mammalian cell cultures during biopharmaceutical production. Biotechnol Bioeng 114:1290–1300. https://doi.org/10.1002/bit.26254.
22. Karp PD, Weaver D, Paley S, Fulcher C, Kubo A, Kothari A, Krummenacker M, Subhraveti P, Weerasinghe D, Gama-Castro S, Huerta AM, Muñiz-Rascado L, Bonavides-Martinez C, Weiss V, Peralta-Gil M, Santos-Zavaleta A, Schröder I, Mackie A, Gunsalus R, Collado-Vides J, Keseler IM, Paulsen I. 2014. The EcoCyc database. EcoSal Plus 6. https://doi.org/10.1128/ecosalplus.ESP-0009-2013.
23. Heeb S, Haas D. 2001. Regulatory roles of the GacS/GacA two-component system in plant-associated and other gram-negative bacteria. Mol Plant Microbe Interact 14:1351–1363. https://doi.org/10.1094/MPMI.2001.14.12.1351.
24. Gao C, Jiang T, Dou P, Ma C, Li L, Kong J, Xu P. 2012. NAD-independent l-lactate dehydrogenase is required for l-lactate utilization in Pseudomonas stutzeri SDM. PLoS One 7:e36519. https://doi.org/10.1371/annotation/83922541-168a-4d4f-846a-cb5d127aa7a9.
25. Bensel T, Stotz M, Borneff-Lipp M, Wollschläger B, Wienke A, Taccetti G, Campana S, Meyer KC, Jensen PØ, Lechner U, Ulrich M, Döring G, Worlitzsch D. 2011. Lactate in cystic fibrosis sputum. J Cyst Fibros 10:37–44. https://doi.org/10.1016/j.jcf.2010.09.004.
26. Fung C, Naughton S, Turnbull L, Tingpej P, Rose B, Arthur J, Hu H, Harmer C, Harbour C, Hassett DJ, Whitchurch CB, Manos J. 2010. Gene expression of Pseudomonas aeruginosa in a mucin-containing synthetic growth medium mimicking cystic fibrosis lung sputum. J Med Microbiol 59:1089–1100. https://doi.org/10.1099/jmm.0.019984-0.
27. Turner KH, Wessel AK, Palmer GC, Murray JL, Whiteley M. 2015. Essential genome of Pseudomonas aeruginosa in cystic fibrosis sputum. Proc Natl Acad Sci U S A 112:4110–4115. https://doi.org/10.1073/pnas.1419677112.
28. Jo J, Cortez KL, Cornell WC, Price-Whelan A, Dietrich LE. 2017. An orphan cbb_3-type cytochrome oxidase subunit supports Pseudomonas aeruginosa biofilm growth and virulence. Elife 6:e30205. https://doi.org/10.7554/eLife.30205.
29. Belenguer A, Duncan SH, Calder AG, Holtrop G, Louis P, Lobley GE, Flint HJ. 2006. Two routes of metabolic cross-feeding between Bifidobacterium adolescentis and butyrate-producing anaerobes from the human gut. Appl Environ Microbiol 72:3593–3599. https://doi.org/10.1128/AEM.72.5.3593-3599.2006.
30. Ramsey MM, Rumbaugh KP, Whiteley M. 2011. Metabolite cross-feeding enhances virulence in a model polymicrobial infection. PLoS Pathog 7:e1002012. https://doi.org/10.1371/journal.ppat.1002012.
31. Lorenz A, Pawar V, Häussler S, Weiss S. 2016. Insights into host-pathogen interactions from state-of-the-art animal models of respiratory Pseudomonas aeruginosa infections. FEBS Lett 590:3941–3959. https://doi.org/10.1002/1873-3468.12454.
32. Starkey M, Rahme LG. 2009. Modeling Pseudomonas aeruginosa patho-

genesis in plant hosts. Nat Protoc 4:117–124. https://doi.org/10.1038/nprot.2008.224.
33. Mahomed TG, Kock MM, Ehlers MM. 2015. Gram-negative bacteria in cystic fibrosis, p 822–831. *In* Méndez-Vilas A (ed), The battle against microbial pathogens: basic science, technological advances and educational programs, vol 2. Formatex Research Center, Badajoz, Spain.
34. Høiby N, Bjarnsholt T, Moser C, Jensen PØ, Kolpen M, Qvist T, Aanaes K, Pressler T, Skov M, Ciofu O. 2017. Diagnosis of biofilm infections in cystic fibrosis patients. APMIS 125:339–343. https://doi.org/10.1111/apm.12689.
35. Capizzani CPDC, Caçador NC, Marques EA, Levy CE, Tonani L, Torres LAGMM, Darini ALDC. 2018. A practical molecular identification of non-fermenting gram-negative bacteria from cystic fibrosis. Braz J Microbiol 49:422–428. https://doi.org/10.1016/j.bjm.2017.07.002.
36. Jørgensen KM, Wassermann T, Johansen HK, Christiansen LE, Molin S, Høiby N, Ciofu O. 2015. Diversity of metabolic profiles of cystic fibrosis Pseudomonas aeruginosa during the early stages of lung infection. Microbiology 161:1447–1462. https://doi.org/10.1099/mic.0.000093.
37. Twomey KB, Alston M, An S-Q, O'Connell OJ, McCarthy Y, Swarbreck D, Febrer M, Dow JM, Plant BJ, Ryan RP. 2013. Microbiota and metabolite profiling reveal specific alterations in bacterial community structure and environment in the cystic fibrosis airway during exacerbation. PLoS One 8:e82432. https://doi.org/10.1371/journal.pone.0082432.
38. Rahme LG, Stevens EJ, Wolfort SF, Shao J, Tompkins RG, Ausubel FM. 1995. Common virulence factors for bacterial pathogenicity in plants and animals. Science 268:1899–1902. https://doi.org/10.1126/science.7604262.
39. Bertani G. 2004. Lysogeny at mid-twentieth century: P1, P2, and other experimental systems. J Bacteriol 186:595–600. https://doi.org/10.1128/JB.186.3.595-600.2004.
40. Shanks RMQ, Caiazza NC, Hinsa SM, Toutain CM, O'Toole GA. 2006. *Saccharomyces cerevisiae*-based molecular tool kit for manipulation of genes from Gram-negative bacteria. Appl Environ Microbiol 72:5027–5036. https://doi.org/10.1128/AEM.00682-06.
41. Lequette Y, Greenberg EP. 2005. Timing and localization of rhamnolipid synthesis gene expression in Pseudomonas aeruginosa biofilms. J Bacteriol 187:37–44. https://doi.org/10.1128/JB.187.1.37-44.2005.
42. Hoang TT, Karkhoff-Schweizer RR, Kutchma AJ, Schweizer HP. 1998. A broad-host-range flp-FRT recombination system for site-specific excision of chromosomally-located DNA sequences: application for isolation of unmarked *Pseudomonas aeruginosa* mutants. Gene 212:77–86. https://doi.org/10.1016/S0378-1119(98)00130-9.
43. Schreiber K, Boes N, Eschbach M, Jaensch L, Wehland J, Bjarnsholt T, Givskov M, Hentzer M, Schobert M. 2006. Anaerobic survival of Pseudomonas aeruginosa by pyruvate fermentation requires an Usp-type stress protein. J Bacteriol 188:659–668. https://doi.org/10.1128/JB.188.2.659-668.2006.
44. Cornell WC, Morgan CJ, Koyama L, Sakhtah H, Mansfield JH, Dietrich LEP. 2018. Paraffin embedding and thin sectioning of microbial colony biofilms for microscopic analysis. J Vis Exp https://doi.org/10.3791/57196.
45. Dietrich LEP, Price-Whelan A, Petersen A, Whiteley M, Newman DK. 2006. The phenazine pyocyanin is a terminal signalling factor in the quorum sensing network of Pseudomonas aeruginosa. Mol Microbiol 61:1308–1321. https://doi.org/10.1111/j.1365-2958.2006.05306.x.
46. Langmead B, Salzberg SL. 2012. Fast gapped-read alignment with Bowtie 2. Nat Methods 9:357–359. https://doi.org/10.1038/nmeth.1923.
47. Li H, Handsaker B, Wysoker A, Fennell T, Ruan J, Homer N, Marth G, Abecasis G, Durbin R, 1000 Genome Project Data Processing Subgroup. 2009. The sequence alignment/map format and SAMtools. Bioinformatics 25:2078–2079. https://doi.org/10.1093/bioinformatics/btp352.
48. Robinson JT, Thorvaldsdóttir H, Winckler W, Guttman M, Lander ES, Getz G, Mesirov JP. 2011. Integrative genomics viewer. Nat Biotechnol 29:24–26. https://doi.org/10.1038/nbt.1754.